Ionics (2016) 22:389–404
DOI 10.1007/s11581-015-1546-4

ORIGINAL PAPER

Electrical, structural, and morphological studies of honeycomb-like microporous zinc-ion conducting poly (vinyl chloride)/poly (ethyl methacrylate) blend-based polymer electrolytes

C. M. Sai Prasanna[1] · **S. Austin Suthanthiraraj**[1]

Received: 2 July 2015 / Revised: 31 July 2015 / Accepted: 30 August 2015 / Published online: 16 September 2015

Abstract Solid polymer electrolytes (SPEs) based on poly (vinyl chloride)/poly (ethyl methacrylate) [PVC/PEMA] blend complexed with zinc triflate [$Zn(CF_3SO_3)_2$] salt have been prepared using solution casting technique. Thin film samples containing various blend ratios of PVC/PEMA with fixed composition of salt have been examined by means of complex impedance analysis, and as a consequence, the typical composition corresponding to PVC (30 wt%)/PEMA (70 wt%) has been identified as the optimized blend exhibiting the highest room temperature ionic conductivity of 10^{-8} Scm^{-1}. The ionic conductivity of the optimized blend was further enhanced from 10^{-8} to 10^{-6} Scm^{-1} by adding the chosen salt in different weight percentages at 301 K. The occurrence of complexation of the polymer blend and an evidence of interaction of cations, namely Zn^{2+} ions with the polymer blend, have been confirmed by Attenuated total reflectance-Fourier transformed infrared (ATR-FTIR) spectroscopy measurement studies. The efficacy of ion-polymer interactions was estimated by means of an evaluation of transport number data pertaining to Zn^{2+} ions which was found to be 0.56. The apparent changes resulting in the structural properties of these polymer electrolytes possessing a honeycomb-like microporous structure were identified using X-ray diffraction (XRD) and scanning electron microscopic (SEM) studies. Such promising features of the present polymer blend electrolyte system appear to suggest possible fabrication of new rechargeable zinc batteries involving improved device characteristics.

✉ C. M. Sai Prasanna
saaimurali3@gmail.com

S. Austin Suthanthiraraj
suthan98@gmail.com

[1] Department of Energy, University of Madras, Guindy Campus, Chennai 600025, India

Keywords Polymer blends · Zinc triflate · Ionic conductivity · ATR-FTIR · XRD · Electron microscopy

Introduction

The design and development of ion conducting polymers by complexing polar polymers with alkali metal salts offer an energetic area of study in materials research. Being light weight and flexible, the research on solid polymer electrolytes has received a tremendous attention in recent years as it is likely to offer a series of potential candidates for advanced solid-state electrochemical devices such as batteries, electrochromic displays, fuel cells, and smart windows [1]. In the battery industry, solid polymer electrolytes have several advantages over conventional liquid electrolytes due to their ability to purge the problem of leakage in highly toxic liquid electrolyte configurations. The success of employing solid polymer electrolytes in power sources is mainly due to wide operating temperature range, feasibility of enhancement in ionic conductivity, large electrochemical stability window, low volatility, and superior structural stability features as well [2].

The earliest and most extensively investigated solid polymer electrolyte towards development of lithium batteries was based on poly (ethylene oxide) PEO due to its ability to form stable complexes with salt-based cations and form a homogenous matrix. However, the major shortcoming aspect of PEO is that it tends to crystallize, exhibiting an appreciably high ionic conductivity only above its melting temperature [3]. Since it has been widely accepted nowadays that the elastomeric amorphous phase of polymers primarily contributes to the significant transport of ions, much effort has been taken by research workers to investigate amorphous polymers exhibiting high room temperature ionic conductivity with exceptional mechanical properties [4]. In addition to this

exploration, blending of polymers is one of the most feasible techniques employed to design polymer electrolytes with an extensive variety of physico-chemical properties [5]. The electrical and physical properties of blended polymer electrolyte film may be improved by realizing a phase-separated electrolyte comprising of first phase adopted to absorb the electrolyte active species, and the second phase providing toughness to the polymer electrolyte films. Polymer blending offers collective advantages like simple method of preparation and has an effective influence over the physical properties of an individual polymer by compositional changes which aid in the enhancement of ionic conductivity [6, 7].

From the wide-ranging group of polymer blends, those blends containing poly (vinyl chloride) (PVC) are among the most significant from both scientific and commercial points of view [8]. The presence of lone pair of electrons at chlorine atom in poly (vinyl chloride) (PVC) facilitates the dissolution of inorganic salts easily, and the mechanical strength of the polymer backbone may be further improved by the dipole–dipole interactions occurring between hydrogen and chlorine atoms [9]. Thus, the PVC-rich phase acts as a good mechanical stiffener with an easy processability and has gained an increased recognition in recent years due to the inexpensive cost and compatibility with many polymers. Even though these appealing properties attribute to the widespread application of PVC, the major drawback in using PVC as a host polymer is that polymer electrolytes based on PVC usually possess low ionic conductivity values at room temperature [10].

The inherent problem of poor ionic conductivity of PVC at ambient temperature may be circumvented by suitably blending PVC with another polymer such as poly (ethyl methacrylate) (PEMA) which has drawn the interest of many groups of researchers by its remarkable properties. It has been reported [11] that PEMA, as a host, has an ionic conductivity of the order of 10^{-3} Scm^{-1} and electrochemical stability window of 4.3 V. Moreover, the carboxylic (−COOH) group of the polymer improves the interconnecting pathways, thereby assisting the movement of ions through polymer segments and confinement of close packing of the chains by large pendant group essentially provides free volume within the polymer matrix [12]. The methacrylic ester in the chemical structure of PEMA provides an excellent chemical resistance, fine surface resistivity, and good mechanical properties [13]. Based on the above facts, PVC and PEMA polymers have been blended together to synchronize each other.

The electrical property of PVC/PEMA blends may be properly customized by adding different inorganic salts as a dopant, depending on their reactivity with the host polymer matrix. PVC and PEMA contain lone pair of electrons that could easily coordinate with cations from inorganic salts, thereby forming polymer–salt complexes and hence providing ionic conduction. Most of the energy storage devices employ lithium-based salts for the fabrication of batteries because of its high specific capacity and excellent cyclic stability. Eventually, such systems suffer from major drawbacks because they are relatively expensive and also have safety concerns, owing to their highly reactive nature [14]. In order to overcome these drawbacks, nowadays, rechargeable batteries, based on zinc triflate salt, are receiving much attention since they are known to be less toxic, easily available owing to its high natural abundance, Zn^{2+} ions having comparable size with Li^{+} ions and safety problems associated with zinc is also minimal and may be handled easily. In addition, triflate anions ($CF_3SO_3^{-}$) were found to yield certain interesting and finer aspects of the conduction mechanism. It has also been quite apparent from global literature that studies on solid polymer electrolytes based on zinc batteries have not been extensively reported and are scanty [15].

Zakaria et al. [16] reported the respective electrical conductivity (σ) values for pure PVC and pure PEMA polymers to be 1.36×10^{-12} and 1.92×10^{-10} Scm^{-1} whereas for the PVC/PEMA blended film, the conductivity value was found to get improved to 4.74×10^{-10} Scm^{-1}. Amir et al. [17] reported that the ionic conductivity of PEMA/PVC blended polymer electrolytes based on NH_4I salt (40 wt%) was of the order of 10^{-6} Scm^{-1} at room temperature whereas Ramesh et al. [2] reported the ionic conductivity of PMMA/PVC blended polymer electrolytes doped with 10 wt% lithium based salt as 1.6×10^{-8} Scm^{-1}. The ionic conductivity of PVC/PEMA blended polymer electrolytes may be further improved to the order of 10^{-3} Scm^{-1} with the addition of additives like plasticizers and fillers which are absent in presently existing system but proposed as a forthcoming research work. The novelty of polymer electrolytes based on PVC/PEMA blend comprising propylene carbonate (PC) as a plasticizer was earlier proposed for lithium battery applications by Rajendran et al. [11] and the mechanical strength of PVC/PEMA-based polymer electrolyte was reported by Hae-SooK-Han et al. [18] to be much higher than that of PVC/PMMA-based polymer electrolyte system.

In the light of these facts, during the present work, PVC and PEMA have been blended together in different weight ratios whereas the weight ratio of $Zn(OTf)_2$ salt remaining fixed in all the systems so as to identify the compatible ratio of the polymer blend, exhibiting the highest room temperature ionic conductivity. Based on the end result, structural and electrical properties in addition to morphological behaviour of the optimized blend (PVC: PEMA) system with different concentrations of zinc triflate salt have been examined and the results are discussed in detail.

Experimental

Materials

Poly (vinyl chloride) (PVC) with a molecular weight 233,000, poly (ethyl methacrylate) (PEMA) with a molecular weight

515,000, inorganic dopant salt, zinc trifluoromethanesulfonate [zinc triflate, $Zn(OTf)_2$] $Zn(CF_3SO_3)_2$ with a molecular weight 363.53 were procured from Sigma-Aldrich, USA. Prior to the preparation, $Zn(OTf)_2$ salt was dried at 100 °C for 1 h to eliminate trace amount of water content present within the material while polymers including PVC and PEMA were used as received. Figure 1 shows the structural formulae for PVC, PEMA and $Zn(OTf)_2$ materials.

Methods of preparation

Zinc ion-conducting solid polymer electrolytes consisting of various blend ratios (10:90, 20:80, 30:70, 40:60, 50:50, 60:40, 70:30, 80:20, 90:10) of PVC/PEMA complexed with fixed 10 wt% $Zn(OTf)_2$ salt were prepared by using the well-known solution casting technique. The weight ratio of polymer blend to $Zn(OTf)_2$ salt is fixed as 90:10. Table 1 shows the details of composition, designation, and room temperature ionic conductivity of [PVC-PEMA- $Zn(OTf)_2$]-based blended polymer electrolytes. Appropriate composition of PVC and PEMA with fixed 10 wt% $Zn(OTf)_2$ was dissolved in 25 ml of a common solvent namely DMF (*N–N* dimethyl formamide), and these mixtures were stirred continuously for several hours at room temperature in order to obtain a homogenous viscous solution. Such solution was then solvent cast into different glass petri dishes and dried in vacuum at 60 °C for 24 h. Thin films thus obtained were further dried at room temperature inside a desiccator for 2 days to remove any excess trace of solvent. Eventually, mechanically stable and free standing films were employed for further investigations.

The same experimental procedure stated previously was reiterated with a view to prepare the optimized blend system containing different concentrations of $Zn(OTf)_2$ salt with the general configuration [PVC: PEMA (optimized blend system)]: *x* wt% $Zn(OTf)_2$ (where x=10, 15, 20, 25, 30, and 35 respectively).

Characterization techniques

The complex impedance measurements for all the samples were carried out using a computer-controlled Hewlett-Packard Model HP 4284A Precision LCR Meter in the frequency range 1 MHz–20 Hz with an excitation signal of 50 mV at ambient temperature. The built-in computer software was used to perform such measurements with precision and calculates both the real and imaginary parts of the impedance values of blended solid polymer electrolyte samples sandwiched between two identical circular and smooth polished stainless steel (SS) blocking electrodes with the test cell configuration [SS/SPE/SS]. The room temperature ionic conductivity of each polymer electrolyte sample was calculated from the measured value of its bulk resistance (R_b) obtained from impedance Cole-Cole plot (Z' vs. Z'') and dimensions of the polymer film as given by the equation:

$$\sigma = \frac{t}{R_b \cdot A} \tag{1}$$

where t is the thickness (cm), R_b the bulk resistance (Ω), and A is the known surface area (cm^2) of the polymer electrolyte samples.

The vibrational modes of the polymer blends and its complexes were characterized by Attenuated total reflectance-Fourier transform infrared spectroscopy (ATR-FTIR) which is a well-established research tool to investigate ion–polymer interaction and possible conformational changes in the host polymer matrix due to the addition of salt. The ATR-FTIR spectra of zinc triflate salt, pure polymers, polymer blend, and their complexes were recorded at room temperature utilizing Perkin Elmer Spectrum-two spectrometer in the wavenumber range 4000 to 400 cm^{-1} with a wavenumber resolution of 2 cm^{-1}. The samples were positioned on the horizontal face of the internal reflectance crystal of Zinc Selenide (ZnSe) where total internal reflection occurred along the crystal–sample interface.

The zinc ionic transport number of the best conducting sample of optimized blend system was examined by collective AC impedance and DC potentiostatic polarization techniques as proposed by Evans et al. [19]. These measurements were carried out by sandwiching solid polymer electrolyte samples between symmetrical zinc reversible non-blocking electrodes according to the following cell configuration:

$$Zn \,/\, PS5 \,/\, Zn \tag{2}$$

Using the computer controlled Hewlett-Packard Model HP 4284A Precision LCR Meter, the initial resistance (R_0) of the cell before polarization was measured in the frequency range 1 MHz–20 Hz. The dependence of the dc current as a function of time for an applied potential of 200 mV (ΔV) was

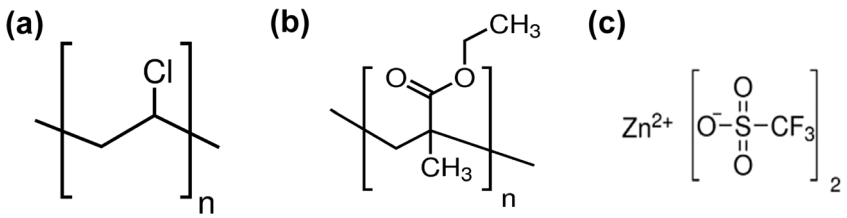

Fig. 1 Structural formulae for **a** PVC, **b** PEMA, and **c** $Zn(OTf)_2$

Table 1 Designation, composition, and room temperature ionic conductivity of [PVC-PEMA- $Zn(OTf)_2$]-based blended polymer electrolytes

Designation	Composition of PVC:PEMA: $Zn(OTf)_2$					Room temperature ionic conductivity σ / Scm^{-1}
	PVC		PEMA		$Zn(OTf)_2$	
	wt/g	wt%	wt/g	wt%	wt/g	
SPE1	0.045	10	0.405	90	0.05	4.54×10^{-9}
SPE2	0.09	20	0.36	80	0.05	4.62×10^{-8}
SPE3	0.135	30	0.315	70	0.05	7.18×10^{-8}
SPE4	0.18	40	0.27	60	0.05	6.79×10^{-8}
SPE5	0.225	50	0.225	50	0.05	5.71×10^{-8}
SPE6	0.27	60	0.18	40	0.05	4.56×10^{-8}
SPE7	0.315	70	0.135	30	0.05	3.77×10^{-8}
SPE8	0.36	80	0.09	20	0.05	2.58×10^{-8}
SPE9	0.405	90	0.045	10	0.05	1.77×10^{-8}

measured by means of a Keithley 6517A electrometer at room temperature. The initial dc current (I_0) was noted and monitored until the steady-state current (I_s) was reached. An AC impedance measurement was carried out after polarization in order to determine the final resistance (R_s) of the cell. The value of $t_{Zn^{2+}}$ was calculated according to the equation,

$$t_{Zn^{2+}} = \frac{I_s(\Delta V - I_0 R_0)}{I_0(\Delta V - I_s R_s)} \quad (3)$$

where I_0 and I_s are the initial and steady state currents, ΔV is the applied dc voltage to the cell, and R_0 and R_s are the resistances of the configured cell before and after polarization.

The amorphous nature of the optimized blend system with various compositions of zinc triflate salt was investigated using X-ray diffraction. The XRD patterns of pure polymers, zinc triflate salt, optimized polymer blend, and its complexes were recorded by means of an XPERT PRO X-ray diffraction system and scanned with the monochromatic CuKα radiation of wavelength λ=1.54 Å at 45 kV and 30 mA ratings with the step size of 0.2° over a bragg angle (2θ) range of 10°–70° at room temperature.

The surface morphology of SPE specimens at room temperature was characterized by means of a VEGA3 SBU Model scanning electron microscope with electron beam energy of 11 kV. The SEM image of the cross-section of the polymer electrolyte film was prepared by cryofracturing the film in liquid nitrogen. The insulating samples were coated with a thin layer of gold by vacuum sputtering for 25 s in order to prevent electrostatic charging.

Results and discussion

AC impedance spectroscopy

Figure 2 shows the variation of ionic conductivity observed in the case of [PVC-PEMA-10 wt% $Zn(OTf)_2$] blended polymer electrolyte system as a function of weight percentage of PVC at room temperature. It is inferred that the ionic conductivity of the polymer matrix increases with an increase in the PVC content to the best possible level, and beyond this level, it decreases. From Table 1, the system SPE3 has been identified as the best conducting polymer blend system with the maximum ionic conductivity of 7.18×10^{-8} Scm^{-1} at room temperature among different blended systems. The observed increase in the ionic conductivity with an increase in the PVC content up to 30 wt% may be due to the effect of long range Coulombic forces which result in the re-dissociation of solvated ion pairs. This aspect would further increase the concentration and segmental mobility of free mobile charge carriers, thus increasing the ionic conductivity too. As the concentration of PVC increases beyond 30 wt%, the conductivity decreases due to the dominating effect of the short range ion-solvent interaction, thereby reducing the effective number of charge carriers available for migration. In addition, as the PVC content increases, the diffusion of ions in the electrolytic system is restricted by PVC-rich phase that is acting like a solid medium and hence the transport of ions through an indirect movement along a convoluted pathway is restricted to PEMA-rich phase which would be responsible for the decrease in the ionic conductivity value [20].

Moreover, with higher concentrations of PVC, high potency of cross-linkage between PVC and PEMA may cause polymer chain entanglements which would lead to the increase in the viscosity. As a consequence, the mobility of charge carriers is likely to get reduced [21].

The ionic conductivity of the optimized blend system SPE3 was then analyzed as a function of different concentrations of salt as depicted in Fig. 3 with the series of corresponding Cole-Cole plots containing the configuration viz. [PVC: PEMA (30 wt%: 70 wt%)]: x wt% [Zn $(CF_3SO_3)_2$] (where x =10, 15, 20, 25, 30, and 35 wt% respectively) shown as the inset. In general, the performance of ion conducting solids with blocking electrodes is characterized by an impedance plot

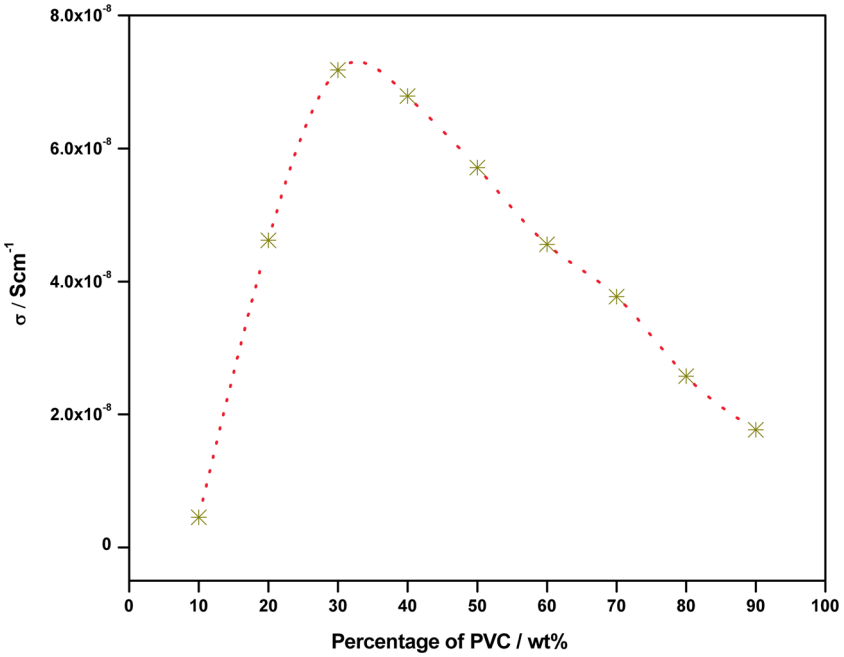

Fig. 2 Variation of ionic conductivity of [PVC-PEMA-10 wt% $Zn(OTf)_2$] blended polymer electrolyte system as a function of weight percentage of PVC at room temperature

with two definite regions consisting of a high frequency semicircle followed by a low-frequency inclined spike. High-frequency semicircle signifies the parallel combination of bulk resistance and bulk capacitance whereas the inclined spike at lower frequency region implies the formation of double layer capacitance due to space charge polarization effects occurring at the electrode–electrolyte interface [22]. In the present study also, from each Nyquist plot (Z' vs. Z'') of zinc ion conducting solid polymer blended electrolytes, it is evident that broadened semicircles in the high frequency region followed by a low-frequency spike are observed and the bulk (ionic) resistance (R_b) of these thin film polymer blend electrolytes may be calculated from the intercept of high-frequency semicircle on the real axis.

The dependence of ionic conductivity on varying salt concentration for the system SPE3 specifies definite interactions between the polymer matrix and salt. The magnitude of the ionic conductivity of the polymer electrolyte is given by:

$$\sigma = \mu_i \cdot n_i \cdot q_i \tag{4}$$

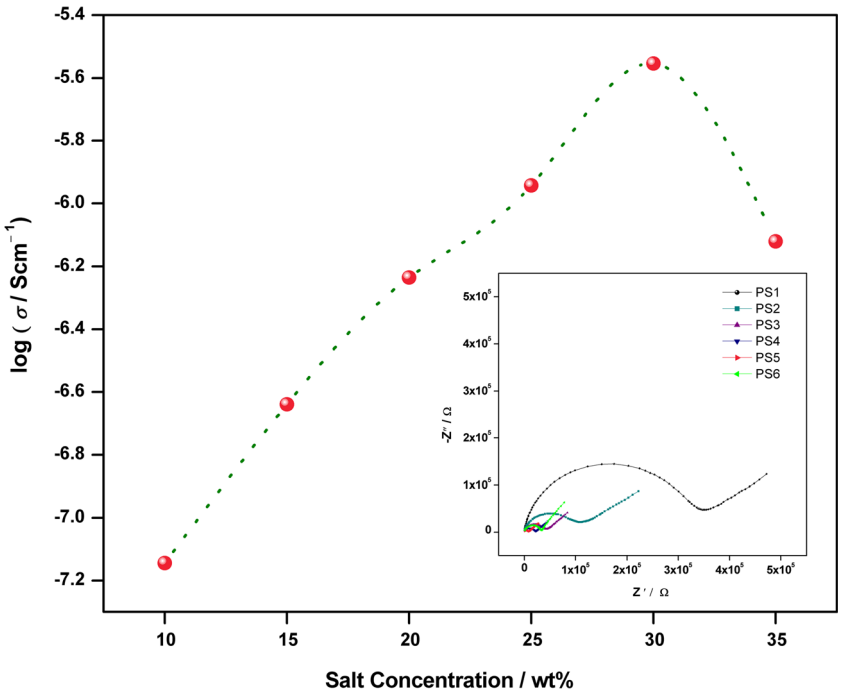

Fig. 3 Variation of the ionic conductivity of the optimized blend system SPE3 as a function of different concentrations of salt with the series of corresponding Cole-Cole plots containing the configuration viz. [PVC: PEMA (30 wt%: 70 wt%)]: x wt% [$Zn(CF_3SO_3)_2$] (where x = 10, 15, 20, 25, 30, and 35 wt% respectively) shown as the inset

where μ_i is the charge carrier mobility, n_i is the concentration of charge carrier, and q_i is the charge of the mobile carrier. Hence, the ionic conductivity may be enhanced by increasing both μ_i and n_i. According to the above equation, it has been observed that the ionic conductivity increases with an increase in the salt concentration to a maximum value of 2.79×10^{-6} Scm^{-1} at 30 wt% loading of zinc triflate salt. It is evident from the inset of Fig. 3 that [PVC(30 wt%): PEMA(70 wt%)]: *x* wt% $Zn(OTf)_2$ (where *x* =10, 15, 20, 25, 30, and 35 wt%) composition of the blended polymer electrolyte displays a decrease in bulk resistance (R_b) by an appreciable change in the diameter of the semicircle up to 30 wt% salt which is then followed by an increase in R_b for higher concentrations of $Zn(OTf)_2$ salt.

The increase in the ionic conductivity of those samples with increase in salt content could be owed to the increase in the number of mobile charge carriers and the amorphous nature of the sample as confirmed from the present XRD data. The increase in the amorphous nature of the polymer film lessens the energy barrier to the segmental mobility of polymer matrix, thereby favouring fast zinc ion transport. For the composition larger than 30 wt% $Zn(OTf)_2$, the fact that ionic conductivity of the electrolyte film decreases could be attributed to the formation of ionic clusters due to aggregation, thereby reducing the number of mobile charge carriers and increasing the viscosity of the polymer solution [23].

Table 2 elucidates the values of ionic conductivity observed for all the complexes of SPE3 system at room temperature and their common designations. Thus, the highest ionic conductivity obtained at room temperature was found to be 2.79×10^{-6} Scm^{-1} for the typical blend system [PVC: PEMA (30 wt%:70 wt%)] containing 30 wt% $Zn(OTf)_2$ and designated as PS5.

ATR-FTIR analysis

ATR-FTIR spectra of zinc triflate salt and pure polymers

The ATR-FTIR spectroscopy is a powerful technique used to examine the complexation behaviour occurring both in crystalline and amorphous phases and interaction between various constituents of a polymer electrolyte structure. In the present study, the ATR-FTIR spectra were recorded for all the samples at room temperature in the transmission mode to establish the nature of interactions occurring between the polymer blend PVC/PEMA (30 wt%:70 wt%) and $Zn(OTf)_2$ salt, and such interactions could bring changes in the vibrational modes characteristic of relevant functional groups of the atoms or molecules of the material [9]. Figures 4, 5a–c, and 6a–e show the ATR-FTIR spectra of pure zinc triflate salt, pure PVC, pure PEMA, PVC/PEMA (30 wt%:70 wt%) blend, PVC/PEMA (30 wt%:70 wt%) blend, and its complexes at ambient temperature. The band assignments for $Zn(OTf)_2$ salt, PVC, and PEMA have already been reported in the literature and cited in Tables 3, 4, and 5, respectively.

Table 2 Values of room temperature ionic conductivity for optimized blend system SPE3 [PVC (30 wt%):PEMA (70 wt%)] : *x* wt% $Zn(OTf)_2$ salt and their designations

x / wt% $Zn(OTf)_2$	Designation (Polymer-Salt)	Weight of $Zn(OTf)_2$ added wt/g	Ionic conductivity at room temperature σ / Scm^{-1}
10	PS1	0.05	7.17×10^{-8}
15	PS2	0.075	2.30×10^{-7}
20	PS3	0.1	5.82×10^{-7}
25	PS4	0.125	1.14×10^{-6}
30	PS5	0.15	2.79×10^{-6}
35	PS6	0.175	7.59×10^{-7}

The symmetric SO_3 stretching vibrational mode [υ_s (SO_3)] of triflate anion ($CF_3SO_3^-$) has been observed at 1033 cm^{-1} in Fig. 4. The peaks noticed at 630 and 523 cm^{-1} correspond to asymmetric SO_3 and CF_3 bending groups [δ_a (SO_3), δ_a (CF_3)]. The band at 768 cm^{-1} may be due to the symmetric bending group (CF_3) of triflate anion [δ_s (CF_3)] whereas the symmetric and asymmetric CF_3 stretching vibrational modes [υ_s (CF_3), υ_a (CF_3)] of the triflate salt are located at 1228 and 1190 cm^{-1}, respectively. The other fundamental characteristic bands of the zinc triflate salt corresponding to OH stretching vibration of adsorbed water, υ(OH) and bending mode of water molecule δ (H_2O) are observed around 3500–3300 and 1651 cm^{-1}, respectively. The IR bands appearing due to water molecules in zinc triflate salt may be attributed to its hygroscopic nature even though the salt has been pre-heated before usage.

Figure 5a shows the characteristic pattern of C–Cl stretching vibrational peaks of PVC in the region 600–700 cm^{-1} which are of complex origin and depend on the conformational structure of the polymer and spatial position of atoms surrounding C–Cl bonds. In addition to this characteristic band structure, the rest part of the spectrum corresponds to different C–C and C–H vibrations too [9]. In the above figure, the typical peak at 684 cm^{-1} may correspond to the C–Cl stretching vibrational mode of PVC. Further, those peaks corresponding to C–H stretching mode appear at 2909, 2937, and 2971 cm^{-1}, whereas CH_2 deformation modes at 1330 cm^{-1}(twisting) and 1426 cm^{-1} (scissoring), CH rocking mode at 1253 cm^{-1}, *trans* CH wagging mode at 959 cm^{-1}, *cis* CH wagging mode at 608 cm^{-1}, and back bone C–C stretching mode at 1094 and 1199 cm^{-1} are also observed.

The ATR-FTIR spectrum of pure PEMA is shown in Fig.5b. In the region from 2900 to 3000 cm^{-1}, the transmittance bands observed at 2982, 2938, and 2906 cm^{-1} may be attributed to the overlapping of C–H stretching vibration of methylene [$C(CH_3)$] and ethylene [$O(C_2H_5)$] groups. The characteristic peaks of PEMA due to the carbonyl C═O stretching [υ(C═O)] and asymmetrical stretching vibrations of C–O–C bond [υ_a (COC)] are observed at 1722, 1237, and 1142 cm^{-1} respectively. The –CH_2 scissoring, –CH_2 wagging, and –CH_2

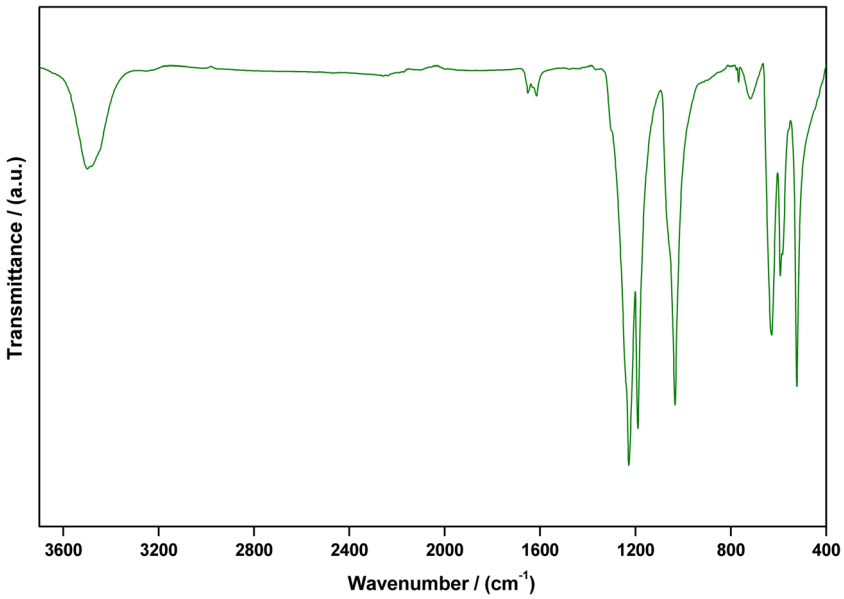

Fig. 4 ATR-FTIR spectrum of pure $Zn(OTf)_2$ at ambient temperature

rocking vibrational frequencies of PEMA are observed at 1479, 941, and 749 cm^{-1}, respectively. Those peaks seen at 1447 and 1387 cm^{-1} may be attributed to the asymmetrical O–C_2H_5 bending [γ_a (OC_2H_5] and CH_2 twisting [τ (CH_2] vibrations of PEMA. The pair of bands ascribable to [υ(CO)] stretching modes of –COO– and –OC_2H_5 groups of PEMA are found to appear at 1267 and 1172 cm^{-1}, respectively, and the band corresponding to strong υ (C–C) stretching mode of ethyl group of PEMA is observed at 1024 cm^{-1}.

Interactions occurring within the PVC/PEMA blend

Interestingly, the blending of PVC with PEMA is found to effectively shift the polymer cage peak frequencies, as shown in Fig. 5c. In the case of PVC/PEMA (30 wt%:70 wt%) blend, the set of peaks due to carbonyl [υ(C═O)] stretching group, asymmetric C–O–C [υ_a (COC)] stretching groups, and υ (C–C) stretching mode of ethyl group from PEMA appear to be shifted to 1724, 1239, 1144, and 1025 cm^{-1} with a lower intensity in proportion to the composition of PEMA (70 wt%) in the blend. The specific interaction occurring between C═O group of PEMA and α-hydrogen of CH–Cl in PVC has been clearly indicated by the observed shift in the vibration band pertaining to C═O group to higher wavenumbers and also by the changes revealed in the intensity of carbonyl stretching peak of PEMA. This observation is similar to those results reported by many researchers [16]. The characteristic peaks found in the case of pure PVC at 608 and 684 cm^{-1} corresponding to *cis* CH wagging and C–Cl stretching vibrations and another one seen at 431 cm^{-1} get

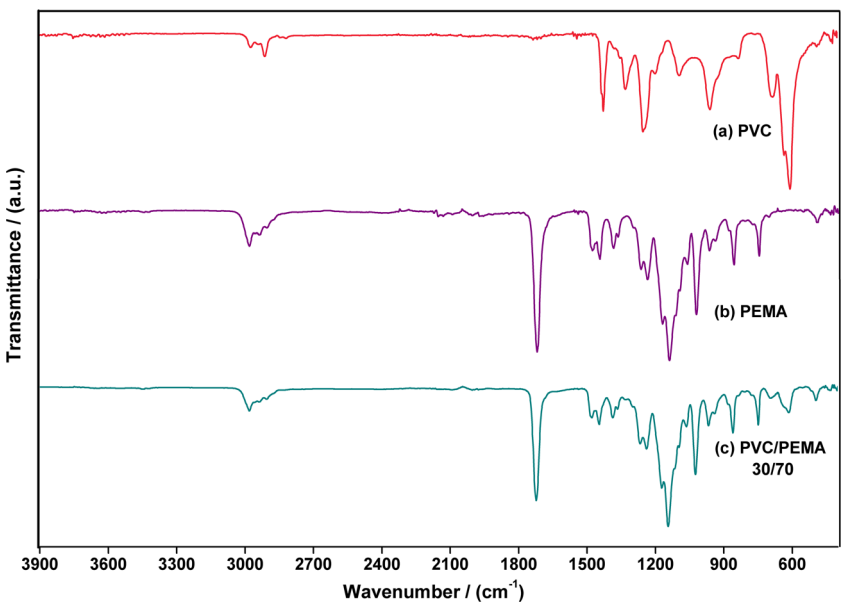

Fig. 5 ATR-FTIR spectra of room temperature **a** pure PVC, **b** pure PEMA, **c** PVC/PEMA (30 wt%: 70 wt%) blend

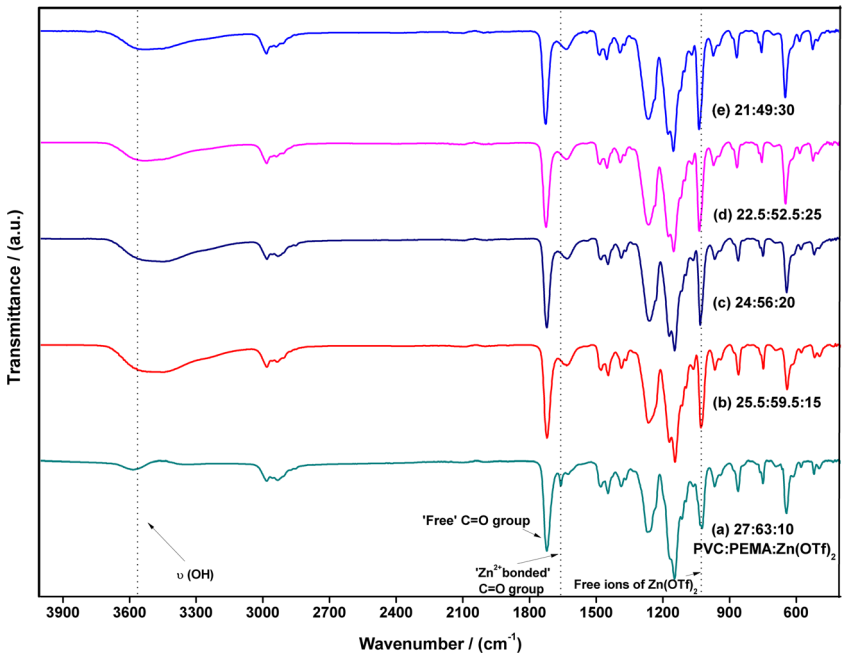

Fig. 6 ATR-FTIR spectra recorded at room temperature for SPE3 system with varying concentrations of zinc triflate salt

shifted to 615, 695, and 435 cm^{-1} respectively in PVC/PEMA blend and emerged with a reduced intensity in proportion to the 30 wt% of PVC in the blend. The fact that the peak of pure PVC at 1330 cm^{-1} corresponding to CH_2 deformation (twisting) mode has changed form a broad peak to a small shoulder peak in the blend and appears at 1332 cm^{-1} with a lesser intensity may be due to the overlapping of this peak with some of the characteristic peaks of PEMA at 1387, 1367, and 1267 cm^{-1}. The deserved changes of the position and intensity of those peaks for the functional groups of C═O, asymmetric C–O–C, υ (C–C) stretching, *cis* CH wagging, C–Cl stretching, and CH_2 deformation (twisting) modes of both PEMA and PVC are indicative of the occurrence of Zn^{2+} ionic interaction with the polymer hosts [26]. In the blended film PVC/PEMA (30 wt%:70 wt%), C–H stretching bands noticed at 2910, 2954, and 2981 cm^{-1} may be due to the overlapping and merging of C–H stretching bands of pure PVC at 2909, 2937, and 2971 cm^{-1} and those of pure PEMA at 2906, 2938, and 2982 cm^{-1} [24]. The occurrence of an interaction between C–H stretching vibrations of PVC and PEMA further signifies that both PVC and PEMA are compatible to form a polymer blend.

Interactions between PVC/PEMA blend and $Zn(CF_3SO_3)_2$ salt

During the present investigation, it is interesting to notice that certain changes in the vibrational spectra of PVC/PEMA blend occur as a consequence of integration with zinc triflate salt in different weight percentages resulting in favourable sites for the coordination of zinc ions within these blended polymer electrolytes. The introduction of zinc triflate salt into the PVC/PEMA blend appears to effectively alter the position of several characteristic bands as revealed from the IR spectra observed in the case of these polymer electrolytes with shifted wavenumbers owing to the fact that the surrounding of the triflate ion changes due to its sensitive approach to the state of coordination [24]. Figure 6a–e shows the existence of triflate ions in all the PVC-PEMA-$Zn(CF_3SO_3)_2$ complexes. PEMA has lone pair of electrons at the oxygen (O) atoms

Table 3 Assignment of IR vibrational modes and wavenumbers exhibited by $Zn(OTf)_2$ salt

Vibrational modes of triflate anion ($CF_3SO_3^-$)	Wavenumber (cm^{-1})	Reference
Symmetric CF_3 stretching vibrational mode υ_s (CF_3)	1231	[24]
Asymmetric CF_3 stretching vibrational mode υ_a (CF_3)	1195	[24]
Asymmetric CF_3 bending group δ_a (CF_3)	574	[25]
Asymmetric SO_3 bending group δ_a (SO_3)	640	[25]
Symmetric CF_3 bending group δ_s (CF_3)	756	[25]
Symmetric SO_3 stretching vibrational mode υ_s (SO_3)	1032	[25]
OH stretching vibration of adsorbed water υ(OH)	3400	[26]
Bending mode of water molecule δ (H_2O)	1660-1590	[26]

Table 4 Assignment of IR vibrational modes and wavenumbers exhibited by PVC

Vibrational modes	Wavenumber (cm^{-1})	Reference
C–Cl stretching	692	[27]
C–H stretching	2890-2958	[28]
CH_2 deformation	1337 (twisting) and 1426 (scissoring)	[29]
CH rocking	1254	[28]
trans CH wagging	959	[28]
cis CH wagging	610	[30]
Back bone C–C stretching	1075, 1192	[31]

located at the carbonyl (C═O) and C–O–C groups while PVC contains lone pair of electrons at the chlorine (Cl) atoms of –CCl groups. This typical carbonyl (C═O) group absorption peak observed over the region 1800 to 1650 cm^{-1} in all these complexes is likely to be highly responsive to ionic interactions which may enable the electropositive species of the salt (i.e., Zn^{2+} cations) to easily coordinate with oxygen atoms of the C═O group which is essentially a strong electron donating group in nature [34]. Figure 7 shows the ATR-FTIR spectra of PVC-PEMA-$Zn(CF_3SO_3)_2$ complexes ranging from 1800 to 1670 cm^{-1} with increasing salt concentrations from 10 to 30 wt% at ambient temperature. The addition of small quantity (~10 wt%) of $Zn(CF_3SO_3)_2$ is found to results in shifting of the C═O band in the case of chosen blend to the lower side of the frequency scale and the corresponding peak slightly gets broadened as well. As the salt concentration increases further from 10 to 30 wt%, a constant lowering in the position of [υ(C═O)] band from 1724 cm^{-1} in the blend to 1720 cm^{-1} (~ 4 cm^{-1}) in the case of various complexes occur along with a methodical broadening of the C═O peak [35]. This type of shifting of [υ(C═O)] band towards lower wavenumbers suggests that Zn^{2+} ions from zinc triflate would coordinate with oxygen atom of the C═O group by sharing its electron density to form C═O ····· Zn^{2+} bond, thus weakening the bond between C and O [24].

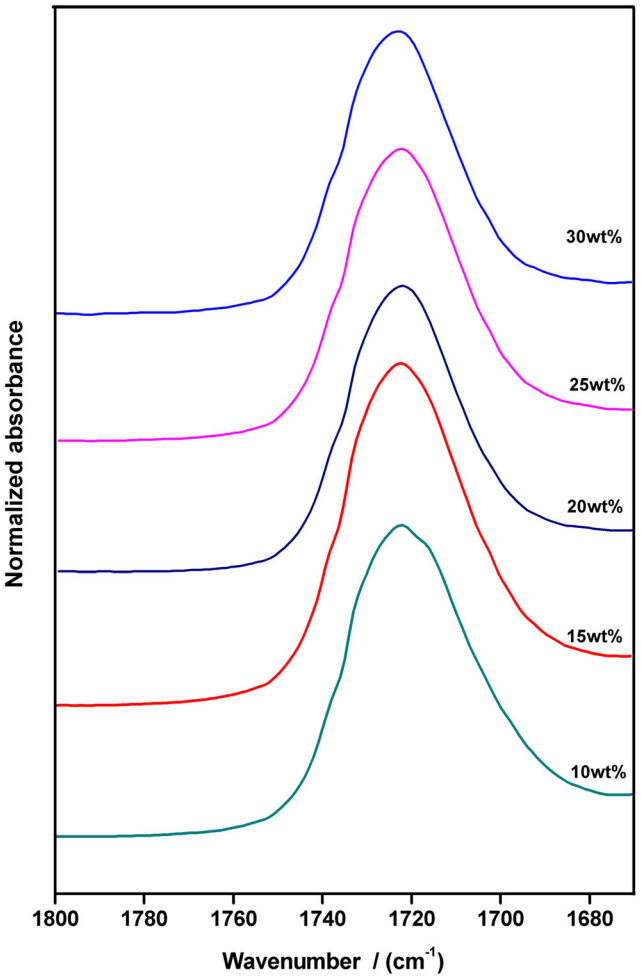

Fig. 7 ATR-FTIR spectra of PVC-PEMA-$Zn(CF_3SO_3)_2$ complexes ranging from 1800 to 1670 cm^{-1} with increasing salt concentrations from 10 to 30 wt% at ambient temperature

In addition to the band located around the region 1724–1720 cm^{-1} due to [υ(C═O)] group, a small new shoulder peak at 1660 cm^{-1} emerges upon addition of 10 wt% salt to the blend which further confirms the coordination of oxygen

Table 5 Assignment of IR vibrational modes and wavenumbers exhibited by PEMA

Vibrational modes	Wavenumber (cm^{-1})	Reference
C-H stretching vibration of methylene C (CH_3) and ethylene O (C_2H_5) groups	2982, 2939, 2910	[31]
C═O stretching [υ(C═O)]	1723	[24]
Asymmetric stretch of C–O–C [υ_a (COC)]	1249, 1142	[24]
–CH_2 scissoring	1485	[32]
–CH_2 wagging	947	[32]
–CH_2 rocking	756	[32]
Asymmetric O–C_2H_5 bending [γ_a (OC_2H_5)]	1446	[24]
CH_2 twisting [τ (CH_2)]	1388	[24]
υ (CO) stretching modes of –COO– group	1265	[24]
υ (CO) stretching modes of –OC_2H_5 group	1175	[24]
υ (C–C) stretching mode of ethyl group	1024	[33]

atoms of C═O group with Zn^{2+} ions, thereby forming an aquazinc cation, ZnH_2O^+ bonded through Zn^{2+}– O interactions. On the other hand, the band at 1660 cm^{-1} ascribable to the bending vibrations of water molecule of zinc triflate salt tends to reveal the presence of a bridging medium between the heteroatom (O) of C═O group in PEMA with Zn^{2+} ions from the chosen salt. All these complexes are found to show such a newborn "Zn^{2+} bonded C═O" absorption band with wavenumbers shifting from 1660 to 1628 cm^{-1} mutually with the peak broadening as the salt content increases from 10 to 30 wt%. The movement of Zn^{2+} ions from one coordination site to another coordination site may be facilitated by the occurrence of such water molecule, thereby enhancing the ionic conductivity of the blended polymer electrolyte systems. This particular newborn shoulder peak was completely absent in the case of pure PVC, pure PEMA, and blended PVC/PEMA films. This feature infers the interaction of Zn^{2+} ions with the oxygen atom (O) of C═O group, thus implying the complete solubility of zinc triflate salt in these blended polymer electrolytes [26, 36]. Such changes noticed in the band position with the increase in salt concentration are a strong evidence of the occurrence of the interaction of the salt with the polymer backbone having the electron rich group [35].

The fact that the O–C_2H_5 asymmetric bending mode [γ_a (OC_2H_5] of PEMA located at 1447 cm^{-1} has no major changes in its band position while varying the salt concentration from 10 to 30 wt% specifies that there may not be any possibility of an interaction of Zn^{2+} ions with these groups of PEMA [37]. Besides, the pair of absorption bands attributed to the different vibration modes of PEMA ester groups and appearing at 1267 cm^{-1} due to υ (CO) stretching modes of –COO– and another one at 1239 cm^{-1} owing to asymmetric C–O–C [υ_a (COC)] groups within the blend which is apparently merged with the symmetric CF_3 stretching mode [υ_s (CF_3)] of $Zn(CF_3SO_3)_2$ originally seen at 1228 cm^{-1} and producing an intense peak at 1269 cm^{-1} for 10 wt% $Zn(OTf)_2$ salt are found to shift towards lower frequency scale from 1269 to 1259 cm^{-1} (~10 cm^{-1}) as the salt concentration increases from 10 to 30 wt% in the polymer blend-salt complexes. This aspect might be due to the interaction of Zn^{2+} ions with the partially negative oxygen of the ester group. The asymmetric stretching vibration of C–O–C bond [υ_a (COC)] in the case of the polymer blend at 1144 cm^{-1} has experienced a shift to higher wavenumbers (~1148 cm^{-1}) as the salt concentration increases from 10 to 30 wt%. As a consequence, comparatively, these observations tend to indicate in explicit terms that Zn^{2+} ions interact more intensely with the ester groups than with C═O group of PEMA since the carbonyl group shifts slightly from its original position (~ 4 cm^{-1}) whereas ester group of PEMA has demonstrated a larger shift (~10 cm^{-1}). However, due to the high polarity of C═O group, the inorganic salt does not necessarily interact with the carbonyl group of the polymers. The tendency of coordination of zinc ions to the asymmetric C–O–C stretching bonds [υ_a (COC)] (ester groups) of PEMA may be assigned to the freedom of rotation about a single bond in contrast to the restricted rotation of the double bonded C═O group. Although there are two lone pairs of electrons as coordination sites in both C═O and asymmetric C–O–C bonds of PEMA that could coordinate with Zn^{2+} ions independently, the rotation about the C–O–C bond has a greater flexibility of exposing the lone pair of electrons to Zn^{2+} ions, thereby facilitating the complexation to occur. The changes witnessed in the wavenumber of the abovementioned bands confirms the coordination of Zn^{2+} ions to the oxygen atoms at both C═O and ester groups of PEMA polymer present in the present polymer blend system [24].

The *cis* CH wagging and C–Cl stretching modes of vibrations pertaining to PVC in the case of the polymer blend seen at 615 and 695 cm^{-1} unite with the strong peak at 630 cm^{-1} due to the asymmetric SO_3 bending group δ_a (SO_3) originating from $Zn(CF_3SO_3)_2$ and resulting in the formation of a sharp peak in almost all the synthesized complexes at wavenumbers around the region 644 to 642 cm^{-1}. The addition of zinc triflate salt from 10 to 30 wt% produces such a significant shift in the vibrational mode of this band accompanied by a marked increase in the intensity of observed peaks. These considerable changes occurring in the intensity and position of the observed peaks imply that suitable interaction has taken place between *cis* CH wagging, C–Cl stretching vibrational bands of PVC, and zinc triflate salt. The shifting of the vibrational peaks could be attributed to the change in environment of C–H bond owing to the coordination of Zn^{2+} cations to the chlorine atoms in PVC [24].

Those characteristic peaks of the blend corresponding to C–H stretching at 2910, 2954, and 2981 cm^{-1} are found to get shifted to 2933, 2957, 2983, 2936, 2958, 2982, 2932, 2958, 2982, 2908, 2938, 2982, 2907, 2938, and 2982 cm^{-1} in the various blends containing 10, 15, 20, 25, and 30 wt% $Zn(OTf)_2$ salt. On the other hand, the characteristic peak of $Zn(CF_3SO_3)_2$ at 3500 cm^{-1} due to υ(OH) and δ (H_2O) vibrational bands gets broadened as the salt concentration increases in polymer blend–salt complexes which may be attributed to the formation of intermolecular hydrogen bonds and to the change in environment for triflate ions ($CF_3SO_3^-$) within the complex [28, 38].

There is a strong peak at wavenumbers around the region 1032 to 1031 cm^{-1} with increased intensities at higher salt content in all the polymer blend–salt complexes, and this might be due to the overlapping of the symmetric stretching vibrational mode of SO_3 [υ_s (SO_3)] which would come from free triflate ions at 1033 cm^{-1} and υ (C–C) stretching mode of ethyl group of PEMA appearing at 1025 cm^{-1} within the blend. The observed increase in the intensity of those peaks around the domain 1032 to 1031 cm^{-1} with an increase in the concentration of the salt accounts for the enhancement in ionic conductivity of PS5 system to 2.79×10^{-6} Scm^{-1}. Since the process of ionic association with triflate anions occurs through SO_3^- end which

is highly receptive to the change in the coordination state of the anion, the overlying multipart spectra noticed in the region 1050–1030 cm^{-1} imply the presence of ion pairs and ion aggregates in addition to free triflate ions [39].

Thus, it is quite evident from the observed changes in the intensity and position of some of the characteristic peaks of PVC/PEMA blend in conjunction with the appearance of characteristic bands arising due to triflate anions that the complexation of the blended polymer PVC/PEMA with zinc triflate salt has occurred.

Transport number data of zinc ions

To evaluate the performance of solid polymer electrolytes (SPE) for rechargeable batteries involving intercalation and de-intercalation of zinc cations throughout the lattice of the host compound, the basic requirement of a high cationic transport number rather than anionic is essential to avoid concentration gradients set up by the mobility of both cations and anions during repeated charging and discharging cycles [40]. The cationic transport number was determined by using the combination of AC impedance spectroscopy and DC polarization method as proposed by Evans et al. [19]. The Zn/PS5/Zn cell was polarized by applying a constant dc potential of 200 mV, and subsequently, the initial and final steady-state currents (I_0 and I_s) after complete polarization of the cell were obtained from the current time plot illustrated in Fig. 8. The measurement of cell resistances (R_0 and R_s) could be accomplished by recording two complex impedance plots as depicted in Fig. 9 in the frequency range 1 MHz–20 Hz before the application of bias potential and after the attainment of steady state. In the present system of solid polymer electrolytes, both Zn^{2+} cations and $CF_3SO_3^-$ anions constitute the potential mobile ionic species.

However, it is realized that the initial current falls with time until a steady-state value is ultimately observed. The migration of both anions and cations towards the zinc electrodes contributes to the initial current value (I_0), but the final steady-state current (I_s) after cell polarization is due to the migration of cations alone. The fall of initial current value until the achievement of steady state is primarily owing to the effect of the growth of passivation layers on the electrodes and formation of a salt concentration gradient across the electrolyte which is caused by the triflate anions being impossible to discharge at the zinc electrodes (Zn electrodes are not reversible vs. anions). This concentration gradient in turn affects the motion of both anions and cations. Once the concentration gradient starts to develop, an electromotive force is generated which appears to act in the opposite direction to the applied field tending to equalize the salt concentration in the electrolyte by the process of diffusion of ions. For the cations, this concentration gradient enhances the overall transport and for anions, the diffusion current opposes the migration current. These two processes of migration of ions under the influence of an external field and diffusion due to concentration gradients are antagonistic and therefore after sufficiently long time, establishment of steady state is reached (i.e., concentration profile resulting from the superposition of both factors remaining stable in time). After the steady state, the current (I_s) flowing from one electrode to another is only due to the motion of cations that could be depolarized and anion motion has been completely ceased. Thus, the significant value of residual current (I_s) confirms Zn^{2+} ionic conduction in the material [19, 41, 42].

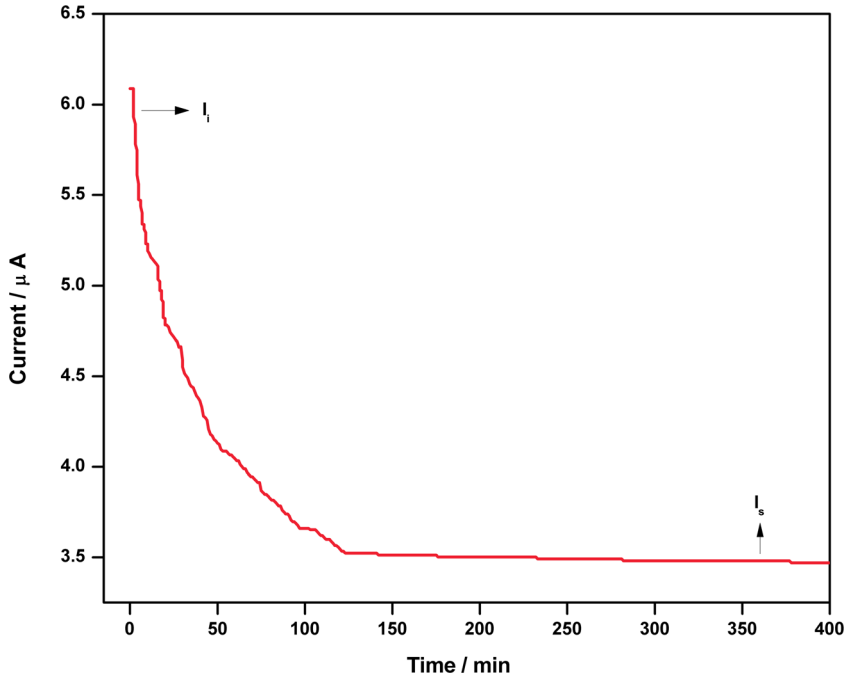

Fig. 8 DC polarization current vs. time plot for Zn/PS5/Zn cell with polarization potential of 0.2 V at ambient temperature

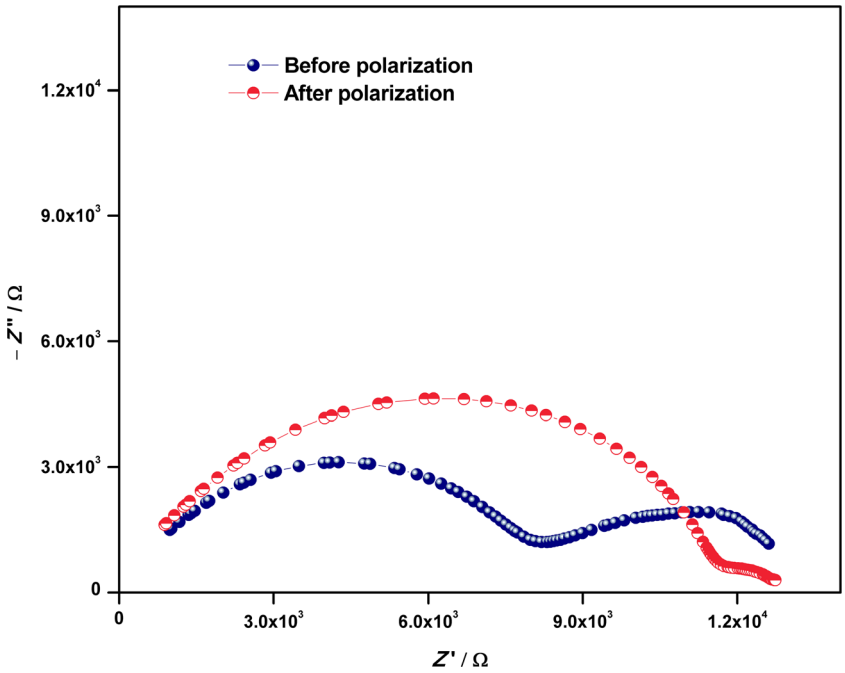

Fig. 9 AC impedance plots before and after polarization of Zn/PS5/Zn cell

Figure 9 shows the set of impedance plots obtained for the abovementioned Zn/PS5/Zn cell at room temperature before and after polarization, and subsequently, from Eq. (3), the value of $t_{Zn^{2+}}$ was found to be 0.56. This fact suggests that the charge transport in these polymer electrolyte films due to zinc ions is quite significant. The reverse polarization could be prevented due to the considerable value of $t_{Zn^{2+}}$, and therefore, the present SPE3 system may be successfully employed to construct batteries for practical applications providing better safety and stability [43]. The appearance of well-defined semicircles in Fig. 9 for the Zn/Zn^{2+}-PS5/Zn cell implies the non-blocking nature of Zn/SPE interface and may be due to the achievement of equilibrium of Zn metal with Zn^{2+} ions within the polymer electrolyte system [44].

X-ray diffraction data

Room temperature X-ray diffraction (XRD) studies have been carried out in order to investigate the effect of zinc triflate salt on the structure of PVC/PEMA blended polymer electrolyte for the system SPE3. Figure 10a– i shows the diffraction patterns obtained for pure PVC, pure PEMA, zinc triflate,

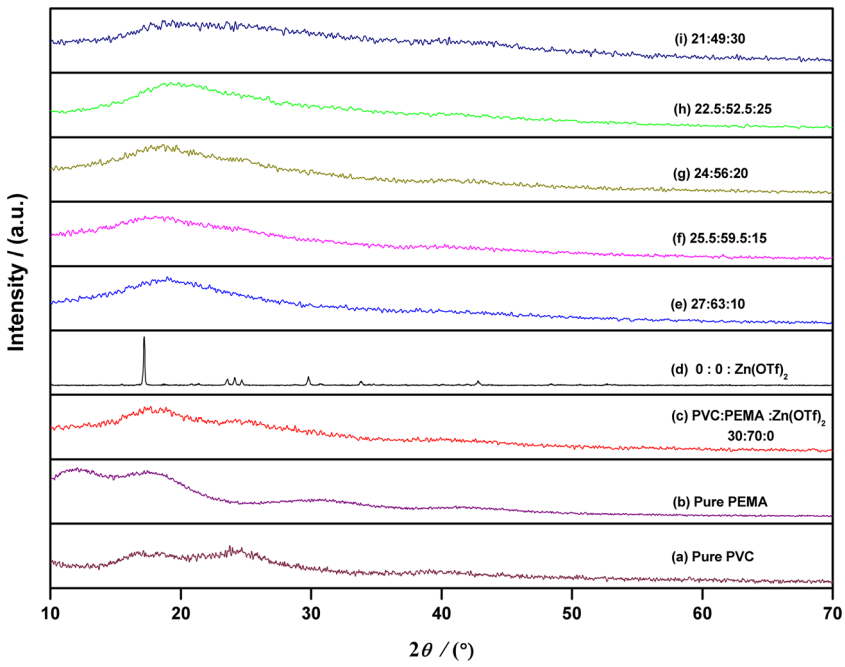

Fig. 10 XRD patterns for **a** pure PVC, **b** pure PEMA, **c** PVC:PEMA (30 wt%:70 wt%) blend system, **d** $Zn(OTf)_2$ salt, **e**–**i** PVC: PEMA (30 wt%: 70 wt%) blend system with 10, 15, 20, 25, and 30 wt% $Zn(OTf)_2$

optimized PVC/PEMA (30:70) blend, and their complexes. The XRD pattern in the case of pure PVC and depicted in Fig. 10a shows two broad humps centered at 2θ=17° and 24° respectively. Meanwhile, the XRD pattern for pure PEMA powder specimen as shown in Fig. 10b is characterized by two halos at 2θ=12° and 18° respectively. The presence of broader Bragg peaks in the case of XRD patterns observed for both pure PVC and PEMA powders illustrates predominant amorphous nature of both the polymers. It has been observed that when PVC is blended with PEMA in the optimized ratio (30 wt%:70 wt%), as shown in Fig. 10c, those peaks corresponding to pure PVC and pure PEMA coalesce and appear as one broad peak at 17.6°, illustrating the presence of interaction such as cross-linking between PVC and PEMA [21].

Figure 10d illustrates the sharp intense characteristic peaks at 2θ=17.2°, 23.5°, 24.1°, 24.6°, and 29.8° revealing the highly crystalline character of zinc triflate salt. It has also been identified from Fig. 10e–i that the addition of $Zn(OTf)_2$ salt in different weight ratios to the optimized polymer blend system SPE3 further increases the amorphous nature of the samples, and this is also evident by the shifting of peaks and reduction in peak intensity associated with the broadening of peaks in all these complexes. The broad peak at 17.6° for SPE3 system has been shifted to 18.9°, 17.3°, 18.6°, 19.8°, and 18.6° for those complexes containing 10, 15, 20, 25, and 30 wt% zinc triflate. The presence of complexation has been further confirmed from an increase in the broad nature of the peak associated with a decrease in peak intensity upon incorporation of the dopant in all the complexes. These broadened peaks may be called amorphous humps which are the typical characteristic features of amorphous materials. Further, those sharp peaks corresponding to crystalline $Zn(OTf)_2$ salt completely disappear in almost all the complexes, thereby indicating the feasibility of an absolute complexation and complete dissolution of $Zn(OTf)_2$ in the present blended polymer electrolytes. The disappearance of crystalline peaks corresponding to pure zinc triflate salt also indicates that these electrolytes are in amorphous region causing a reduction in the energy barrier to the segmental motion of the polymer electrolyte thus facilitating greater diffusion of ions and inducing the highest ionic conductivity as well [45, 46].

Scanning Electron Microscopy

The scanning electron microscopy (SEM) is one of the most versatile instrumental tools to evaluate and examine the microstructure morphology of conducting surfaces. Figure 11a–e presents the SEM images of [PVC (30 wt%)–PEMA (70 wt%)]: $Zn(OTf)_2$ complex for 0, 15, and 30 wt% loading of the salt along with the magnified image and cross-sectional view of the best conducting sample. Figure 11a for the pure optimized blend shows a very smooth, uniform non-porous morphology without any apparent interface between the two polymers confirming the absolute miscibility of the blend system. The change in the smooth morphology of the pure polymer blend and enhancement in ionic conductivity of the blend may be accomplished by the addition of salt. Figure 11b depicts the surface morphology of PS2 with 15 wt% loading of $Zn(OTf)_2$ salt, presenting a wider pore size distribution and exhibiting an irregularity and less periodicity in its arrangement. The ionic conductivity of the prepared samples has increased further for the system PS5 with 30 wt% addition of salt displaying a honeycomb pattern with increase in the number of pores and periodicity. Figure 11c, d illustrates the morphology of PS5 film with its corresponding magnified image respectively. They appear to depict honeycomb-patterned beads with a collection of closely packed air spheres of high porosity. The diameters of the multi-sized beads in SEM image for the system PS5 are found to be in the range 11 to 15 μm.

Such micron-sized spherical porous morphology of these polymer blend electrolytes may be due to the complete evaporation of solvent and shows an evidence of the most probable increase in the amorphous region, accounting for the enhanced ionic conductivity [47]. These inter-connected pores with high porosity tend to provide a good pathway for fast zinc ionic transport. It has also been observed from these SEM micrographs that the irregularity and larger pore size configuration in PS2 sample might be due to the meager interaction between the polymer blend and the salt, thereby inducing a lower ionic conductivity. However, the decrease in pore size with homogenous distribution in PS5 sample implies the proper dissolution of zinc triflate salt in the polymer matrix with no agglomeration and may be attributed to the exceptional complexation between $Zn(OTf)_2$ and PVC/PEMA blend which in turn would support the migration of ions, thereby leading to an enhanced ionic conductivity. The increase in the pores with the increase in salt concentration from PS2 to PS5 films might be due to the migration of higher ions since the prime function of pores is to act as a passage for Zn^{2+} cations during charge-discharge cycle. These features tend to conclude that the size, regularity, and level of porosity are greatly governed by the concentration of the salt added and have a correlation in enhancing the ionic conductivity of these polymer blend electrolytes too [48, 49].

By analyzing the layered cross-sectional photograph of PS5 film, as revealed in Fig. 11e, the inner morphology of the polymer membrane was also found to exhibit a uniform porous structure, thus indicating the formation of a homogenous phase. Further, there was no evidence of phase separation in all the SEM images of blended polymer electrolyte films indicating better interaction and compatibility between the polymer blend and salt. Thus, it is obvious that with such a porous polymer electrolyte system SPE3, certain promising features including high ionic conductivity, a wide electrochemical window, and good thermal stability could be accomplished when suitably applied as a separator in zinc ion batteries [50, 51].

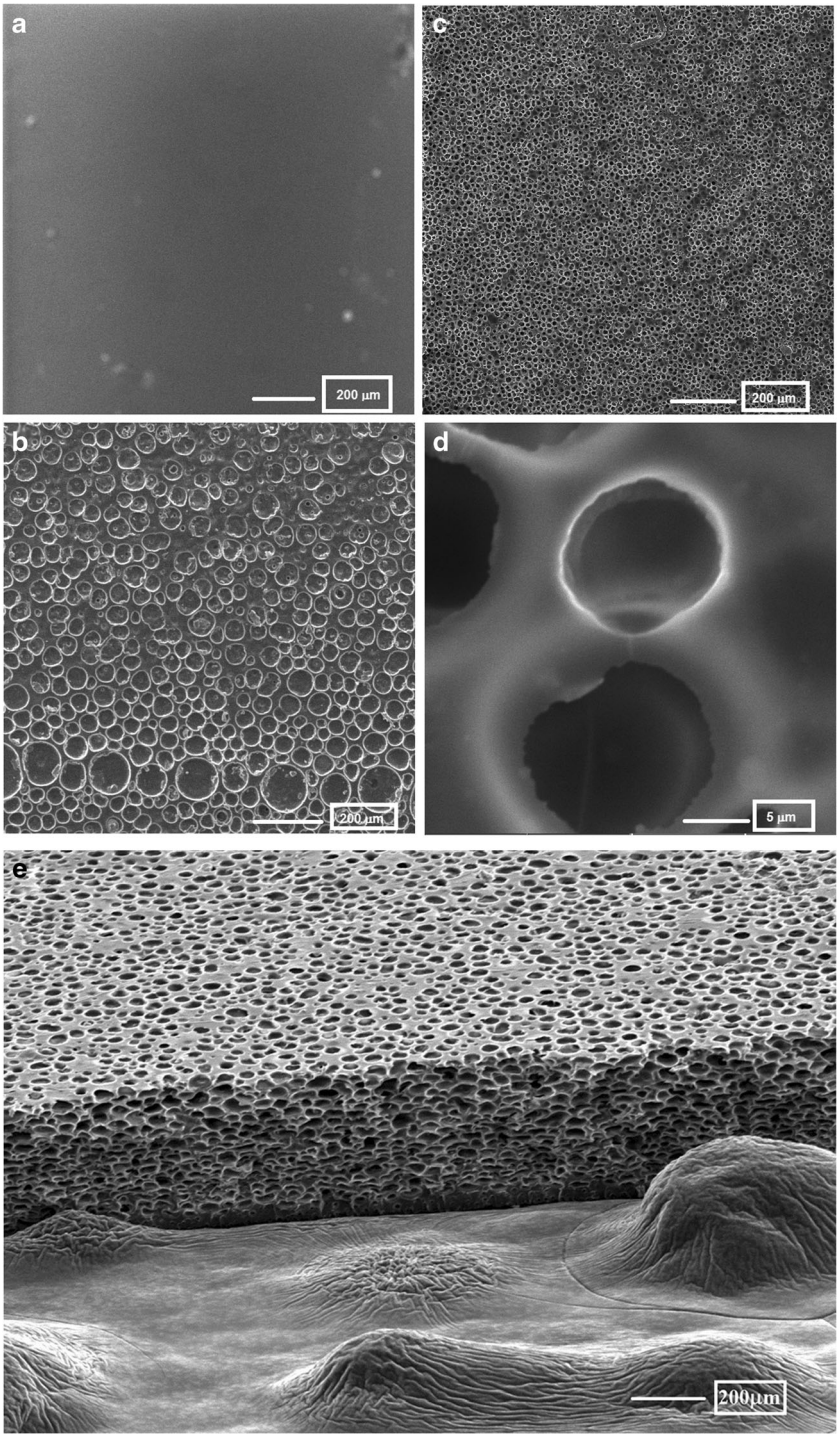

Fig. 11 SEM images of [PVC (30 wt%) - PEMA (70 wt%)]: $Zn(OTf)_2$ complex for **a** 0 wt% $Zn(OTf)_2$ **b** 15 wt% $Zn(OTf)_2$ **c** 30 wt% $Zn(OTf)_2$ **d** its magnified image, and **e** cross section

Conclusion

Zinc ion conducting blended polymer electrolytes based on PVC/PEMA doped with different concentrations of zinc triflate were prepared by solution casting technique. Many characterization techniques were employed to study their electrical, structural, and morphological behaviour. The maximum ionic conductivity of 2.79×10^{-6} Scm^{-1} was observed for the optimized blend system SPE3 [PVC (30 wt%):PEMA (70 wt%)] complexed with 30 wt% zinc triflate at room temperature. There was a strong evidence for the miscibility of the blends as established by ATR-FTIR studies, and the observed changes in the intensity, shape, and position of the peaks have further confirmed the complexation of PVC-PEMA blends with zinc triflate salt. The transport number measurements have been performed in order to confirm the predominant

contribution of zinc cations towards total ionic conductivity. While XRD studies have revealed the amorphous nature of the polymer blend system with an increase in the salt concentration, the porous morphology of the blended polymer electrolyte was recognized by SEM. Thus, the prepared blended polymer electrolytes based on zinc ions under present investigation exhibits better performance and have expected to offer promising applications in energy storage devices.

Acknowledgments One of the authors (C.M.S) of the present work gratefully acknowledges the financial support received in the form of WOS-A programme from the Department of Science and Technology (DST), New Delhi under the DST Sanction No.SR/WOS-A/PS-32/2013 Dated 23.4.2014. The author (C.M.S) would also like to express gratefulness to Dr. N. Rajendran and Mr. K. Pradeep PremKumar, Department of Chemistry, Anna University for their kind help and support in carrying out ATR-FTIR measurements and would also like to thank NCNSNT, University of Madras for SEM analysis.

References

1. Shujahadeen Aziz B, Zul Hazrin Abidin Z (2013) Electrical conduction mechanism in solid polymer electrolytes: new concepts to Arrhenius equation. J Soft Matter. doi:10.1155/2013/323868
2. Ramesh S, Chiam-Wen L (2013) Dielectric and FTIR studies on blending of [xPMMA- (1 - x) PVC] with LiTFSI. Measurement 46: 1650–1656
3. Ugur MH, Toker RD, Kayaman-Apohan N, Gungor A (2014) Preparation and characterization of novel thermoset polyimide and polyimide-peo doped with $LiCF_3SO_3$. eXPRESS Polym Lett 8:123–132
4. Ramesh S, Chai MF (2007) Conductivity, dielectric behavior and FTIR studies of high molecular weight poly(vinylchloride)–lithium triflate polymer electrolytes. Mater Sci Eng B 139:240–245
5. Jacob MME, Prabaharan SRS, Radhakrishna S (1997) Effect of PEO addition on the electrolytic and thermal properties of PVDF-$LiClO_4$ polymer electrolytes. Solid State Ionics 104:267–276
6. Tripathi SK, Gupta A, Kumari M (2012) Studies on electrical conductivity and dielectric behaviour of PVDF-HFP-PMMA-NaI polymer blend electrolyte. Bull Mater Sci 35:969–975
7. Sharma P, Kanchan DK, Gondaliya N, Jayswal M, Joge P (2013) Influence of nano filler on conductivity in PEO-PMMA-$AgNO_3$ polymer blend. Indian J Pure Appl Phys 51:346–349
8. Pielichowski K, Hamerton I (2000) Compatible poly(vinyl chloride)/chlorinated polyurethane blends: thermal characteristics. Eur Polym J 36:171–181
9. Uma T, Mahalingam T, Stimming U (2005) Solid polymer electrolytes based on poly(vinylchloride)-lithium sulfate. Mater Chem Phys 90:239–244
10. Zheng Z, Cao Q, Wang X, Wu N, Wang Y (2012) PVC–PMMA composite electrospun membranes as polymer electrolytes for polymer lithium-ion batteries. Ionics 18:47–53
11. Rajendran S, Ramesh Prabhu M, Usha Rani M (2008) Ionic conduction in poly(vinyl chloride)/poly(ethyl methacrylate)-based polymer blend electrolytes complexed with different lithium salts. J Power Sources 180:880–883
12. Ulaganathan M, Chithra Mathew M, Rajendran S (2013) Highly porous lithium-ion conducting solvent-free poly(vinylidene fluoride-co-hexafluoropropylene)/poly(ethyl methacrylate) based polymer blend electrolytes for Li battery applications. Electrochim Acta 93:230–235
13. Mohammad SF, Zainal N, Ibrahim S, Mohamed NS (2013) Conductivity enhancement of (Epoxidized Natural Rubber 50)/poly(ethyl mathacrylate)-ionic liquid-ammonium triflate. Int J Electrochem Sci 8:6145–6153
14. Tripathi SK, Gupta A, Jain A, Kumari M (2013) Electrochemical studies on nanocomposite polymer electrolytes. Indian J Appl Phys 51:358–361
15. Girish Kumar G, Sampath S (2004) Spectroscopic characterization of a gel polymer electrolyte of zinc triflate and polyacrylonitrile. Polymer 45:2889–2895
16. Zakaria NA, Isa MIN, Mohamed NS, Subban RHY (2012) Characterization of polyvinyl chloride/polyethyl methacrylate polymer blend for use as polymer host in polymer electrolytes. J Appl Polym Sci 126:E419–E424
17. Amir S, Mohamed NS, Subban RHY (2013) Ionic conductivity studies on PEMA/PVC-NH_4I polymer electrolytes. Int J Mater Eng Innov 4:281–290
18. Han H-S, Kang H-R, Kim S-W, Kim H-T (2002) Phase-separated polymer electrolyte based on poly(vinyl chloride)/poly(ethyl methacrylate) blend. J Power Sources 112:461–468
19. Evans J, Colin Vincent A, Peter Bruce G (1987) Electrochemical measurement of transference numbers in polymer electrolytes. Polymer 28:2324–2328
20. Nimma Elizabeth R, Kalyanasundaram S, Gopalan A, Saito Y, Manuel Stephan A (2004) Preparation and characterization of PVC/PMMA blend polymer electrolytes complexed with $LiN(C_2F_5SO_2)_2$. Polimeros 14:1–7
21. Ramesh S, Liew C-W, Morris E, Durairaj R (2010) Effect of PVC on ionic conductivity, crystallographic structural, morphological and thermal characterizations in PMMA-PVC blend-based polymer electrolytes. Thermochim Acta 511:140–146
22. Macdonald JR (1987) Impedance spectroscopy- emphasizing solid materials and systems. John Wiley & Sons, New York
23. Ravi M, Bhavani S, Kiran Kumar K, Narasimaha Rao VVR (2013) Investigations on electrical properties of PVP:KIO_4 polymer electrolyte films. Solid State Sci 19:85–93
24. Sim LN, Majid SR, Arof AK (2012) FTIR studies of PEMA/PVdF-HFP blend polymer electrolyte system incorporated with $LiCF_3SO_3$ salt. Vib Spectrosc 58:57–66
25. Kumar D, Hashmi SA (2010) Ionic liquid based sodium ion conducting gel polymer electrolytes. Solid State Ionics 181:416–423
26. Sim LN, Majid SR, Arof AK (2012) Characteristics of PEMA/PVdF-HFP blend polymeric gel films incorporated with lithium triflate salt in electrochromic device. Solid State Ionics 209–210: 15–23
27. Kulasekarapandian K, Jayanthi S, Muthukumari A, Arulsankar A, Sundaresan B (2013) Preparation and characterization of PVC-PEO based polymer blend electrolytes complexed with lithium perchlorate. Int J Eng Res Dev 5:30–39
28. Ramesh S, Leen KH, Kumutha K, Arof AK (2007) FTIR studies of PVC/PMMA blend based polymer electrolytes. Spectrochim Acta, Part A 66:1237–1242
29. Gherasim CV, Cristea M, Grigoras CV, Bourceanu G (2011) New polymer inclusion membrane. Preparation and characterization. Dig J Nanomater Biostructures 6:1499–1508
30. Subban RHY, Arof AK (2003) Experimental investigations on PVC-LiF_3SO_3-SiO_2 composite polymer electrolytes. J New Mater Electrochem Syst 6:197–203
31. Rajendran S, Ramesh Prabhu M, Usha Rani M (2008) Li ion conduction behavior of hybrid polymer electrolytes based on PEMA. J Appl Polym Sci 110:2802–2806
32. Chithra Mathew M, Karthika B, Ulaganathan M, Rajendran S (2015) Electrochemical analysis on poly(ethyl methacrylate)-based electrolyte membranes. Bull Mater Sci 38:151–156

33. Totolin M, Neamtu I, Filip D, Stoica I, Macocinschi D (2008) An investigation of plasma polymer thin films deposition by low-pressure non-equilibrium plasma. Optoelectron Adv Mater 2:309–314
34. Sownthari K, Suthanthiraraj SA (2013) Synthesis and characterization of an electrolyte system based on a biodegradable polymer. eXPRESS Polym Lett 7:495–504
35. Shukla N, Awalendra Thakur K (2009) Role of salt concentration on conductivity optimization and structural phase separation in a solid polymer electrolyte based on PMMA-$LiClO_4$. Ionics 15:357–367
36. Wu I-D, Chang F-C (2007) Determination of the interaction within polyester-based solid polymer electrolyte using FTIR spectroscopy. Polymer 48:989–996
37. Pradeepa P, Ramesh Prabhu M (2014) Investigations on the addition of different plasticizers in poly(ethylmethacrylate)/poly(vinylidene fluoride-co-hexa fluro propylene) based polymer blend electrolyte system. Int J ChemTech Res 7:2077–2084
38. Jawad MK, Majid SR, Al-Ajaj EA, Suhail MH (2014) Preparation and characterization of poly(1-vinylpyrrolidone-co-vinyl acetate)/poly(methyl methacrylate) polymer electrolyte based on TPAI and KI. Adv Phys Theor Appl 29:14–22
39. Zainol NH, Samin SM, Othman L, Md Isa KB, Chong WG, Osman Z (2013) Magnesium ion-based gel polymer electrolytes: ionic conduction and infrared spectroscopy studies. Int J Electrochem Sci 8:3602–3614
40. Mikrajuddin Abdullah, Wuled Lenggoro, Kikuo Okuyama (2004) Encyclopedia of Nanoscience and Nanotechnology: Nalwa HS (ed) Polymer Electrolyte Nanocomposites. American Scientific Publishers, 8: pp 731-762
41. Peter Bruce G, Colin Vincent A (1987) Steady state current flow in solid binary electrolyte cells. J Electroanal Chem 225:1–17
42. Watanabe M, Tokuda H, Muto S (2001) Anionic effect on ion transport properties in network polyether electrolytes. Electrochim Acta 46:1487–1491
43. Kim Y-S, Cho Y-G, Odkhuu D, Park N, Song H-K (2013) A physical organogel electrolyte: characterized by in situ thermo-irreversible gelation and single-ion-predominant conduction. Sci Rep 3:1–6
44. Girish Kumar G, Sampath S (2005) Electrochemical and spectroscopic investigations of a gel polymer electrolyte of poly(methylmethacrylate) and zinc triflate. Solid State Ionics 176:773–780
45. Ramesh S, Yi LJ (2009) Structural, thermal, and conductivity studies of high molecular weight of poly(vinylchloride)-lithium triflate polymer electrolyte plasticized by dibutyl phthalate. Ionics 15:725–730
46. Rajendran S, Ramesh Prabhu M (2010) Effect of different plasticizer on structural and electrical properties of PEMA-based polymer electrolytes. J Appl Electrochem 40:327–332
47. Ulaganathan M, Nithya R and Rajendran S (2012) Surface Analysis Studies on Polymer Electrolyte Membranes Using Scanning Electron Microscope and Atomic Force Microscope: Viacheslav Kazmiruk (ed) Scanning Electron Microscopy. InTech, Europe, pp 671-694
48. Dong W, Zhou Y, Yan D, Mai Y, Lin H, Jin C (2009) Honeycomb-structured microporous films made from hyperbranched polymers by the breath figure method. Langmuir 25:173–178
49. Ramesh S, Liew C-W (2013) Development and investigation on PMMA-PVC blend-based solid polymer electrolytes with LiTFSI as dopant salt. Polym Bull 70:1277–1288
50. Wong CS, Badri KH, Ataollahi N, Law KP, Su'ait MS, Hassan NI (2014) Synthesis of new bio-based solid polymer electrolyte polyurethane-$LiClO_4$ via prepolymerization method: effect of NCO/OH ratio on their chemical, thermal properties and ionic conductivity. Int J Chem Nuclear, Mater Metall Eng 8:1168–1175
51. Zhang J, Sun B, Huang X, Chen S, Wang G (2014) Honeycomb-like porous gel polymer electrolyte membrane for lithium ion batteries with enhanced safety. Sci Rep 4:1–7